UCRL-JC-127526
PREPRINT

Unexploded Ordnance Detection Using Imaging Giant Magnetoresistive (GMR) Sensor Arrays

Alison Chaiken

This paper was prepared for submittal to the
UXO Forum '97
Nashville, TN
May 27-30, 1997

May 6, 1997

Lawrence Livermore National Laboratory

UNEXPLODED ORDNANCE DETECTION USING IMAGING GIANT MAGNETORESISTIVE (GMR) SENSOR ARRAYS

Alison Chaiken
Mailstop L-350
Lawrence Livermore National Lab
Livermore, CA 94550
chaiken@llnl.gov
http://www.wsrcc.com/alison/magnetism.html
(510) 422-7129

ABSTRACT

False positive detections account for a great part of the expense associated with unexploded ordnance (UXO) remediation. Presently fielded systems like pulsed electromagnetic induction systems and cesium-vapor magnetometers are able to distinguish between UXO and other metallic ground clutter only with difficulty. The discovery of giant magnetoresistance (GMR) has led to the development of a new generation of integrated-circuit magnetic sensors that are far more sensitive than previously available room-temperature-operation electronic devices. The small size of GMR sensors makes possible the construction of array detectors that can be used to image the flux emanating from a ferrous object or from a non-ferrous object with eddy currents imposed by an external coil. The purpose of a GMR-based imaging detector would be to allow the operator to easily distinguish between UXO and benign objects (like shrapnel or spent bullets) that litter formerly used defense sites (FUDS).

In order to demonstrate the potential of a GMR-based imaging technology, a crude magnetic imaging system has been constructed using commercially available sensors. The ability to roughly determine the outline and disposition of magnetic objects has been demonstrated. Improvements to the system which are necessary to make it into a high-performance UXO detector are outlined.

INTRODUCTION

Many techniques are in use or have been proposed for use as UXO detectors. The two most commonly employed technologies are electromagnetic induction detection and fluxgate magnetometry. While time-domain analysis of inductive signals has been suggested as a way to differentiate between hazardous and benign types of buried material, neither the induction detector nor the fluxgate magnetometer may be engineered to produce an image of potential UXO objects. The success of imaging technologies based on arrays of detectors like forward-looking infrared cameras for infrared target identification and charge-coupled device video cameras for consumer applications suggests that the sensor-array paradigm is worth exploring for UXO detection as well. Neither the electromagnetic induction nor fluxgate magnetometry methods is well-suited for incorporation into a detector array since these sensors are bulky in size. Newly developed GMR sensors, on the other hand, are now available now in integrated circuit form. These sensors are attractive for a variety of applications because of their high sensitivity (over ten times greater than Hall sensors), room-temperature operation (unlike SQUID magnetometers) and moderate cost (currently $5 each in small quantities).

Physics of the Giant Magnetoresistance

The giant magnetoresistance (GMR) effect was discovered in France in 1988, but it has been widely investigated by US investigators.[Baibich, 1988] As illustrated in Figure 1, GMR is a very large change in electrical resistance that is observed in a ferromagnet/paramagnet multilayer structure when the relative orientations of the magnetic moments in alternate ferromagnetic layers change as a function of applied field. The basis of the GMR is the dependence of the electrical resistivity of electrons in a magnetic metal on the direction of the electron spin, either parallel or antiparallel to the magnetic moment of the films (indicated by heavy arrows below). Electrons which have a parallel spin undergo less scattering and therefore have a lower resistance. When the moments of the magnetic layers (NiFe in Fig. 1) are antiparallel at low field, there are no electrons which have a low scattering rate in both magnetic layers, causing an increased resistance. At applied magnetic fields where the moments of the magnetic layers are aligned, electrons with their spins parallel to these moments pass freely through the solid, lowering the electrical resistance. The resistance of the structure is therefore proportional to the cosine of the angle between the magnetic moments in

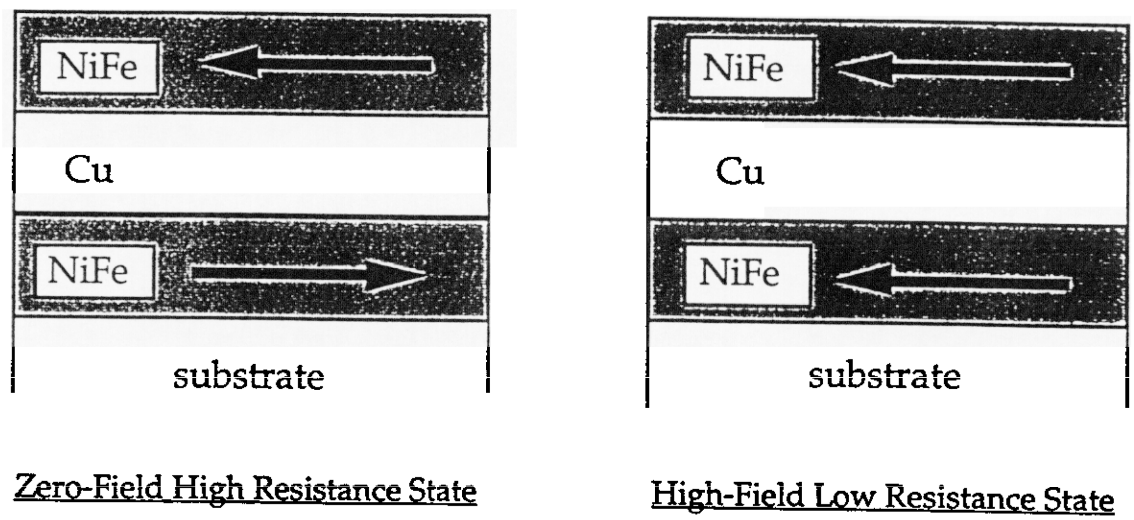

Figure 1. The Giant Magnetoresistance effect is due to the large difference in electrical resistance between two magnetic states of a metallic multilayer film.

adjacent magnetic layers.[Chaiken, 1990]

The occurrence of the GMR effect depends on the ability of the applied magnetic to switch the relative orientation of the magnetic moments back and forth between the parallel and antiparallel states. In some multilayers a quantum-mechanical interlayer exchange coupling across Cu or another paramagnetic metal causes a zero-field antiparallel alignment which can be overcome by a high applied field.[Binasch, 1989] The magnitude of the GMR effect can be surprisingly large, up to 80% at room temperature in Co/Cu multilayers as reported by workers at Sanyo.[Kano, 1993] However, the fields needed to saturate Co/Cu multilayers are too large for sensor applications. Other multilayers are designed to have an antiparallel state in a limited applied field range by alternating ferromagnetic layers (Co and Fe layers instead of two NiFe layers) with different intrinsic switching fields.[Chaiken, 1991] Outputs of GMRs can be as large as 12% at 20 Oe in film form, with slightly lower sensitivity found in microfabricated devices.[Anthony, 1994] The NVE sensors used in this study have an output of only 0.3% at 15 Oe, so considerable improvement is expected in the future.

GMR sensors have recently been evaluatedd for use in geophysical exploration and found to have a noise floor of 0.1 to 1.0 nT in an unshielded, unfiltered system.[McGlone, 1997] This sensitivity is comparable to an electromagnetic induction system, although not at the level of cesium-vapor magnetometer systems. A practical UXO

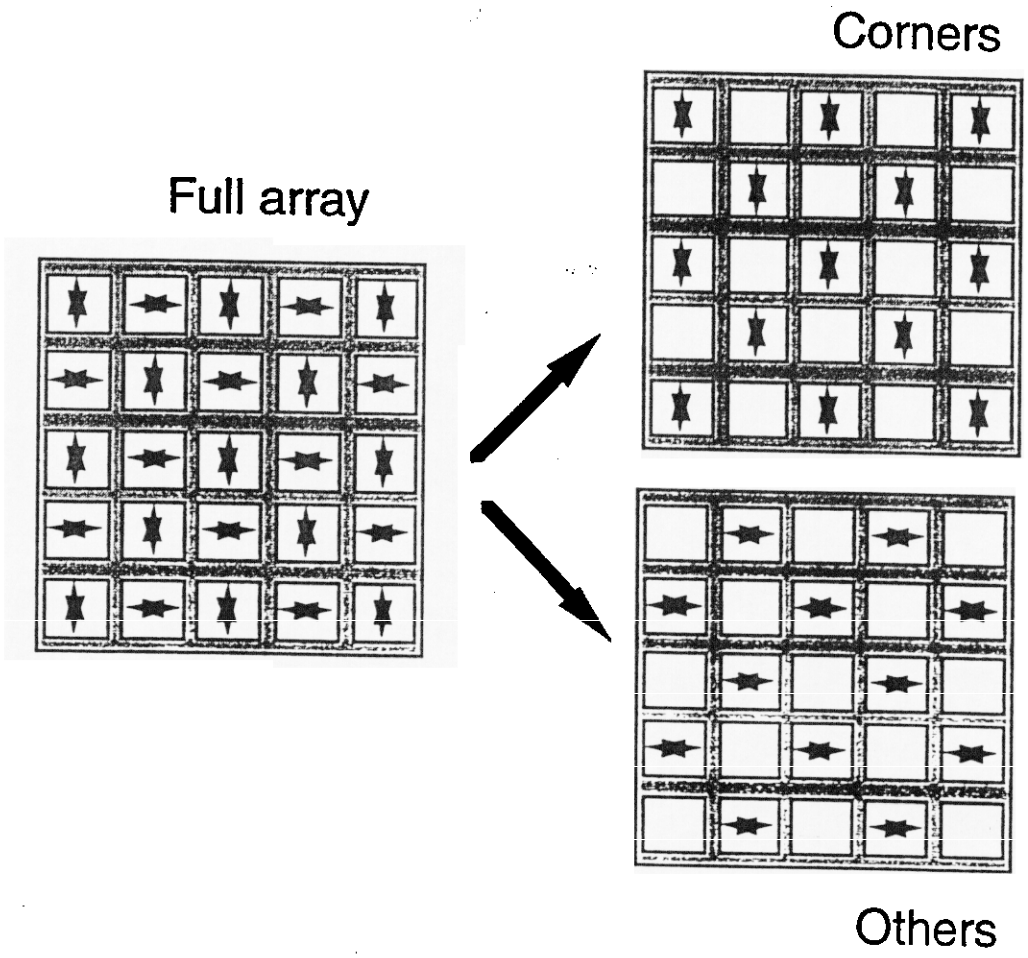

Figure 2. An illustration of the layout of the 5x5 GMR sensor array. Each white square in the "full array" drawing on the left represents one NVE NVS5B15 sensor. The arrows on this drawing indicate the orientation of the axis of sensitivity for each sensor. The right side of the figure shows how the outputs of the elements are split up in the images that follow.

system in the end is expected to incorporate a variety of sensor types integrated into a single package so that maximum sensitivity and imaging capability will be available to operate in concert.

The impact of GMR array UXO detectors on DOD site remediation activities is potentially great. The inspection of false positives during cleanup of contaminated areas adds greatly to the cost and duration of site remediation. Typically, 50 to 60 pounds of scrap metal are recovered for each ordnance item found using present technology. An easy-to-use imaging UXO detection system would allow a relatively inexperienced user to rapidly distinguish between objects. Successful development of an imaging detector for site remediation will provide useful baseline information for design of a battlefield-deployable land or shoreline mine imaging system.

DEMONSTRATION SYSTEM DESIGN

Nonvolatile Electronics' NVS5B15 sensors were employed for this project.[NVE, 1994] NVE is at present the only commercial vendor of GMR sensors, although other electronics companies (for example, Honeywell and Motorola) are expected to offer GMR products in the next few years. GMR sensors detect a single vector component of an applied field, like Hall generators or pulsed inductive detectors, so three orthogonal sensors banks will be

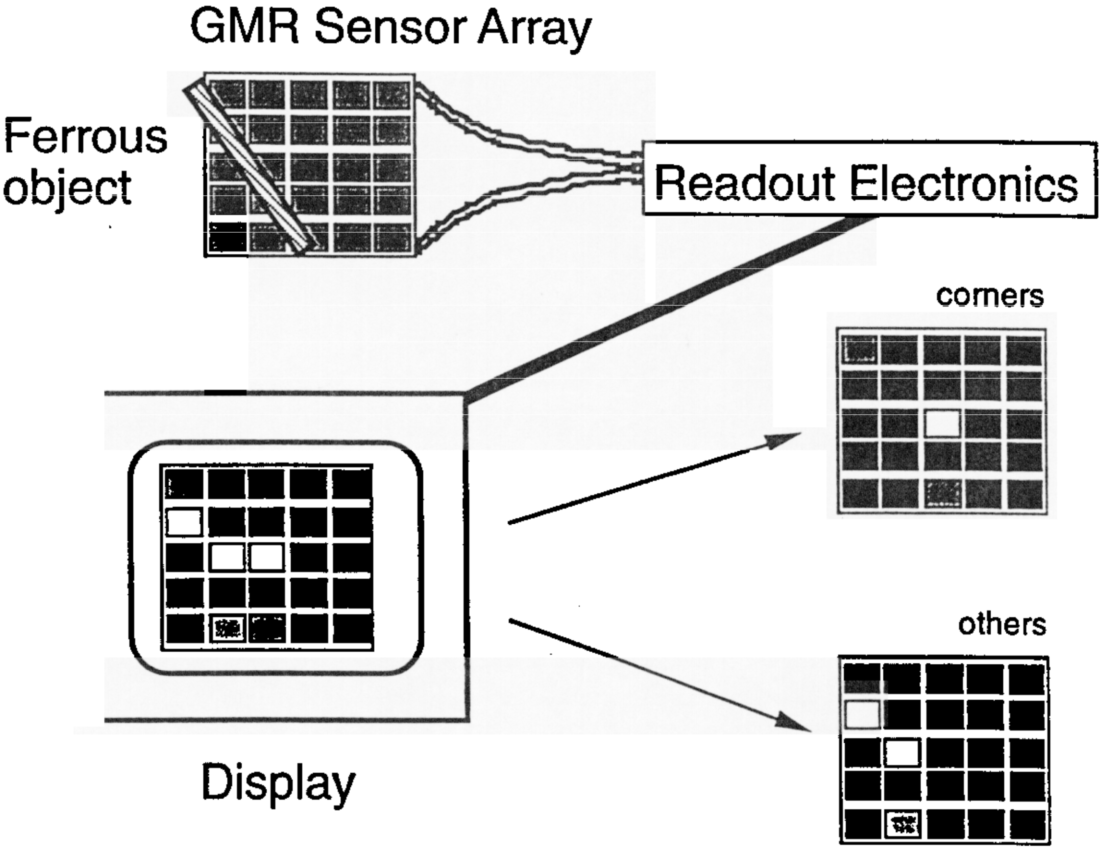

Figure 3. Layout of the image acquisition apparatus.

necessary for full 3D imaging capability. A single 2D array of sensors was selected for this demonstration where alternate sensors have orthogonal axes of sensitivity. The checkerboard layout of the 5x5 array of sensors is illustrated in Figure 2. In order to simplify interpretation of the magnetic images at the end of the report, the outputs from the sensors with vertical and horizontal axes of sensitivity are displayed separately, as illustrated on the right side of the drawing. The performance of the 5x5 sensor array has been compared with a 3x3 array (not shown) where all the elements have the same vertical axis of sensitivity. The 3x3 array uses the same printed circuit board layout as the 5x5 so that the effect of varying the sensor spacing by a factor of two could be determined.

A schematic of the imaging system is shown in Figure 3. The sensor arrays were interfaced with an electronics chassis that contained a 15V and 5V power supply. The outputs of the sensors were connected to a National Instruments 64-channel data acquisition card which was installed in a Pentium PC. National Instruments' LabView software was used to acquire the images that follow. The images are unprocessed beyond resizing and adjustment of the grayscale for printability. Since there are only 25 sensors per image, the data files are only 400 bytes (25 sensors x 16 bits per sensor) in size. Each image is an average of 1000 readouts of the full array during a 10-second period (acquisition rate = 100 Hz), although there is no reason that data could not be acquired much more rapidly (10-100 kHz). 1000 readouts of the array was decidedly overkill; images were not degraded by the averaging of smaller data sets.

A variety of ferrous objects were imaged. These included tools, bolts, nails, rebar and permanent magnets. All objects were imaged in their remanent magnetic state (i.e., no external applied field) except where otherwise specifically noted. Before an image was acquired, the no-object output of all the sensors was obtained using the PC. This background signal represents a combination of offsets in the sensors, the sensors' response to the earth's field (no magnetic shielding was used) and their response to magnetic objects in the laboratory where the data was acquired, e.g. rebar in the floor. This background signal was saved to a file and then subtracted from subsequent data. Objects to be imaged were placed typically 1.5 cm above the sensor array on a lexan stand. The falloff of the signal from the array with separation was studied by stacking firebricks between the array and the ferrous object. Larger objects such as rebar could be detected at a meter separation (signal:background ratio of 2:1) although there was no real image at that separation with the 12cm-square array used for this demonstration.

RESULTS

A sampling of images produced with the GMR sensor array is shown in Figures 4-7. Figure 4 shows an image of a #10 threaded rod 1.5 cm above the array, as pictured in the top-view drawing on the right. The two gray-scale images on the left are data obtained from the sensor array. The top image shows data from the GMR elements (labelled "corners") with a vertical axis of sensitivity. In the "corners" image, a value of 0 volts is displayed at the positions corresponding to the elements with a horizontal axis of sensitivity. The bottom image, labelled "others," shows data from the GMR elements with a horizontal axis of sensitivity. In the "others" image, the positions corresponding to the "corners" elements are displayed as 0 volts. Comparison with Figure 1 will clarify which pixels are meaningful in the two images. In a real UXO detection system, more sophisticated software would combine the two images in a contour or vector plot. Here darker grays indicate higher magnetic flux, while lighter grays indicate lower magnetic flux. The scale is on the right of each image. The numbers next to the grayscale are the sensor signal in volts, so that 1.4e-2 means 14 mV of signal.

In the top image of Figure 4, the magnetic poles on the ends of the rod are being picked up by the sensors at the upper right and lower left corners. In the bottom image, the sensors are responding to magnetic flux leaking from the sides of the rod. While the characteristics of the rod are not completely clear with this low spatial resolution, its general shape and size of the rod can readily be determined.

Figure 5 shows another image of the same rod, only this time flipped over so that it is pointing towards the opposite corners of the array. The movement of the magnetic poles to the upper left and lower right corners is obvious in both images. There are several reasons why this image is not a perfect mirror of Figure 4, namely different lateral placement of the rod on the array and different rotation of the rod about its own axis. The magnetic domains in the rod may not be azimuthally symmetric, with the result that the image may depend somewhat on which side of the rod is facing downward. The rod in Figure 5 is also oriented differently with respect to the earth's field than in Figure 4. In a real UXO system possible ambiguity created by different remanent states of objects can be addressed through application of a rotating alternating-current magnetic field created by two orthogonal sets of coils. A field large enough to force magnetic poles on each surface of a permeable object will make each surface visible to the GMR array, which is in essence a magnetic edge detector.

Figure 6 now shows an image of the same rod in a constant 6 Oe external applied field which was generated with air-core Helmholtz coils. Before acquiring the image, the background of the array was characterized in the presence of the 6 Oe field. The most striking part about this image is that it looks much like Figure 4, showing that the GMR sensor array is able to image ferrous objects even in the presence of a substantial background magnetic field (about fifteen times the

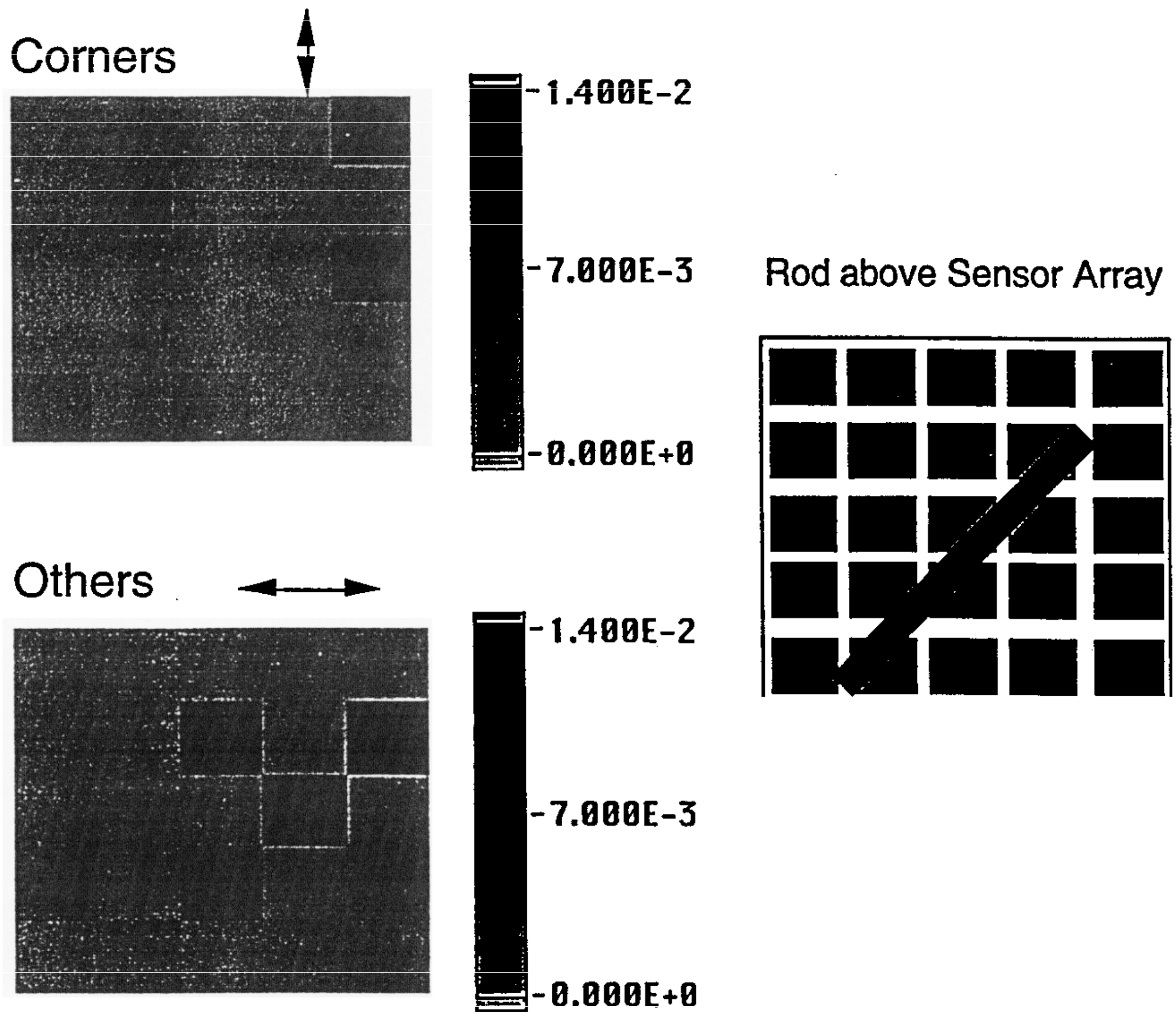

Figure 4. Image of a threaded #10 rod placed above the GMR array. On the left, the gray-scale images show the response of the elements to the magnetic field emanating from the rod. The "corners" image shows only data from the elements with a vertical axis of sensitivity, while the "others" image shows data from the elements with a horizontal axis of sensitivity.

earth's field). The reason for the similarity of the two images is that the array detects spatial magnetic field variations, not the scalar magnetic field amplitude like a cesium-vapor magnetometer. Figure 4 supports the assertion that array-based detectors will usable with magnetic soils as long as the ground clutter is reasonably homogeneous on the length scale of the objects to be detected.

Another point about Figure 6 is that the image is a bit clearer than in Figure 4, where no external field is applied. The improved image quality occurs because much of the flux from the applied field passes through the magnetically soft rod. A more complete outline of the rod could be made by acquiring another image with an applied field in the orthogonal in-plane direction. In fact, a real UXO system would likely incorporate 3 sensor arrays, each with a different orthogonal axis of sensitivity. Data would be read out from each array while a coil applying a magnetic field along that direction is energized. A fully realized system would incorporate a rotating magnetic field and synchronous acquisition from the 3 orthogonal arrays. An additional group of 3 sensors could be used with a portable GMR detector to eliminate noise due to motion of the detector in the earth's magnetic field. (Such a noise-elimination scheme has recently been described for a fluxgate vector magnetometer system by Allen *et al.*[Allen, 1996])

Figure 7 illustrates the ability of the array to image slightly more complex objects. Here two bolts have been placed 1.5 cm above the array. The "corners" image shows substantial flux from the threaded part of the bolt, while the "others" image shows a more difficult to interpret pattern of flux possibly arising from complex domain patterns in the bolt head. The overall "V" symmetry of the objects is apparent in both images. The image of the two bolts would be greatly improved by application of a rotating external field and by a higher resolution array, with more pixels on each object.

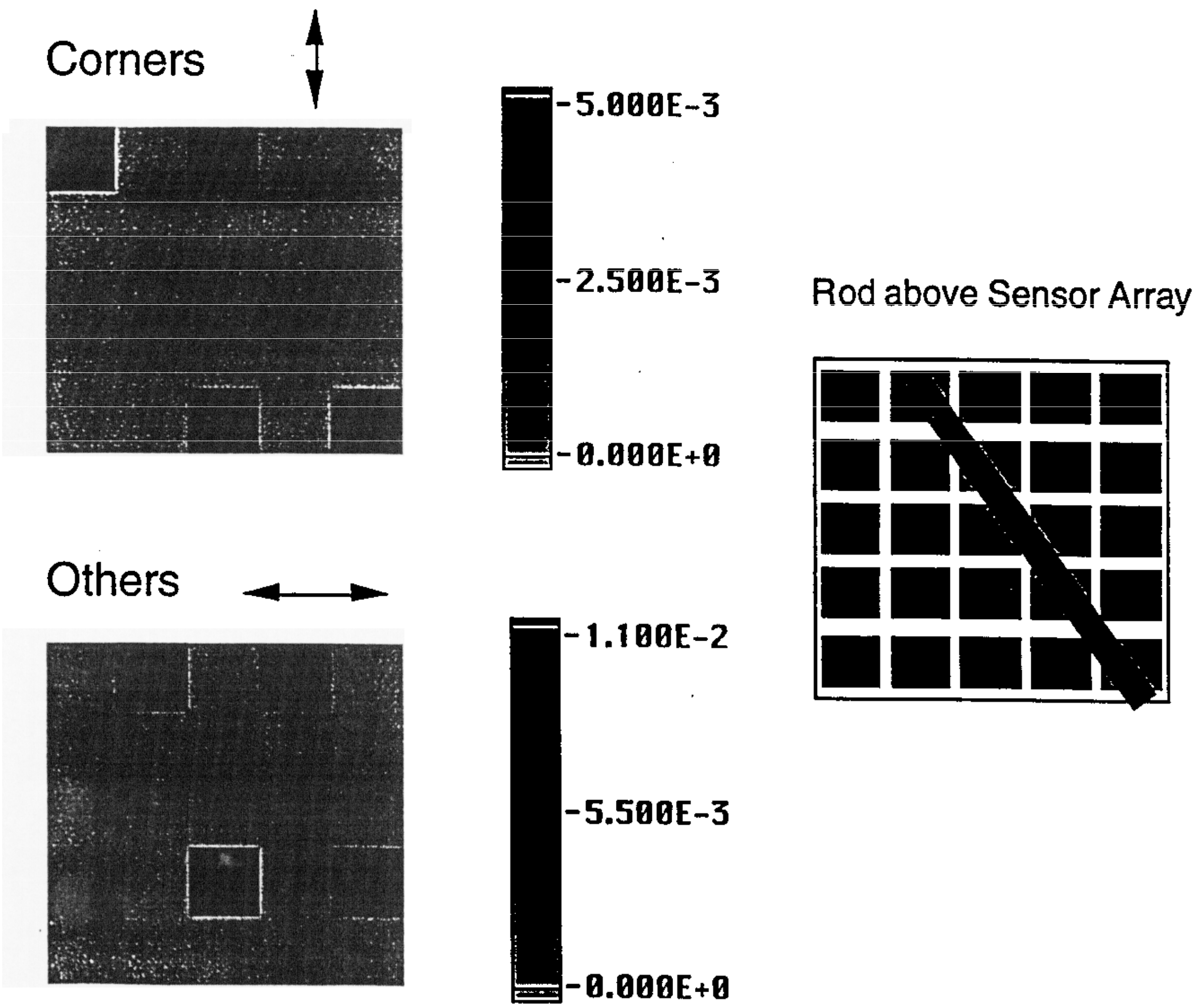

Figure 5. Same as Figure 4, but with the rod flipped about a vertical axis. The image is almost a mirror reversal of Figure 4.

Another study was done to follow the evolution of images as a magnetized object (here a length of 3/4" rebar rod) is moved away from the array. When the rebar was close to the array, it blinded the detector, saturating most of the sensors. As the rebar was moved from 1.5 cm to 9 cm separation, the signal level was reduced from 280 mV to 210 mV, still well above the typical background level of 20-50 mV. The two images at different separation (not shown) demonstrate that we have an object with a vertical axis of symmetry. The image formed by the sensors with their axis of sensitivity parallel to the rebar axis has the same qualitative features independent of spacing. In contrast, the image with the orthogonal axis of sensitivity varies dramatically as a function of spacing. This variation is due to different spatial falloff of

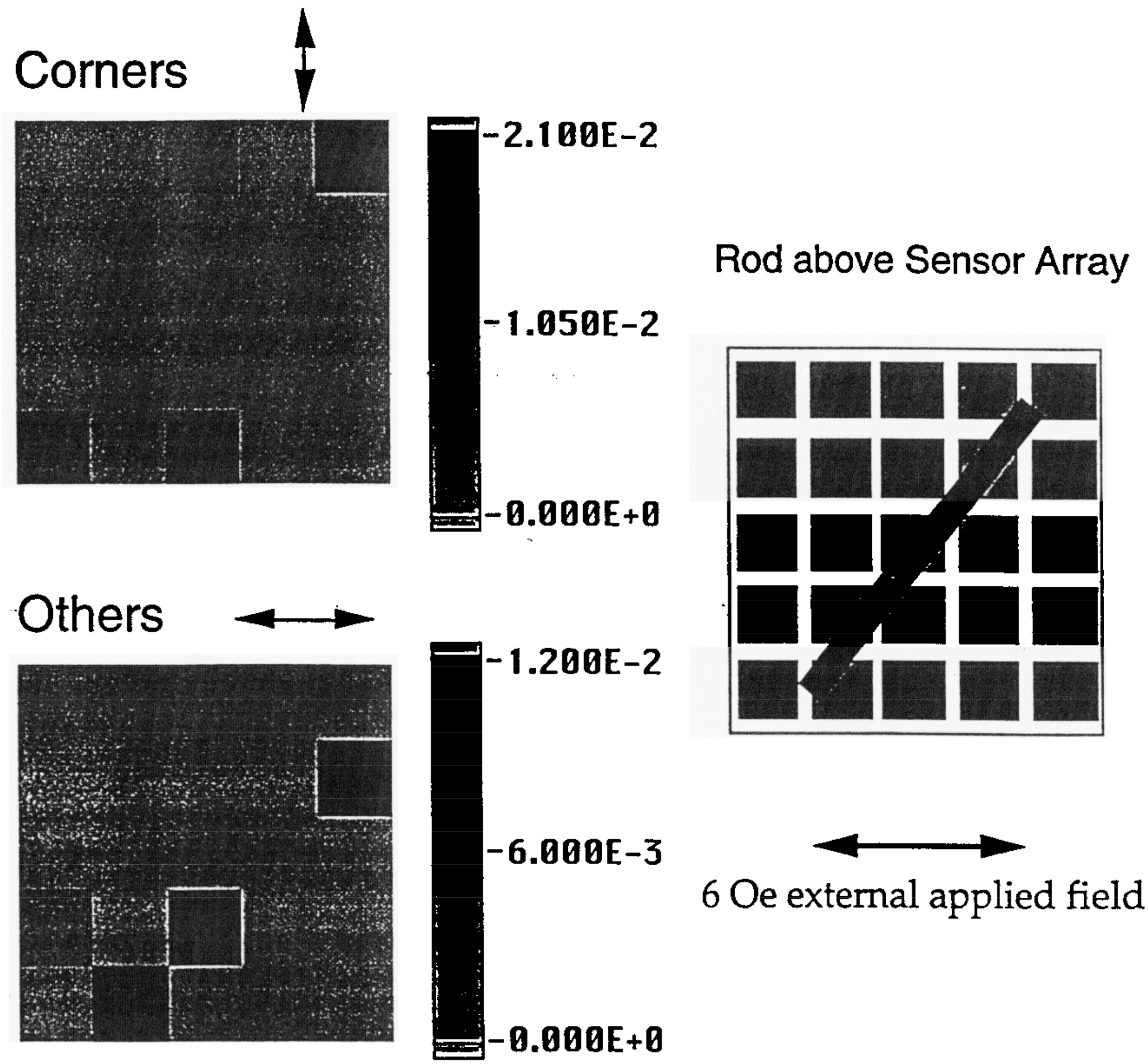

Figure 6. Same as Figure 4, but with a 6 Oe external applied field acting on the rod and the array. The image looks similar to Figure 4 and is even a bit clearer despite the necessary subtraction of the background signal from the external field. This image suggests that GMR arrays will be able to locate ferrous objects even in magnetic soils of volcanic origin.

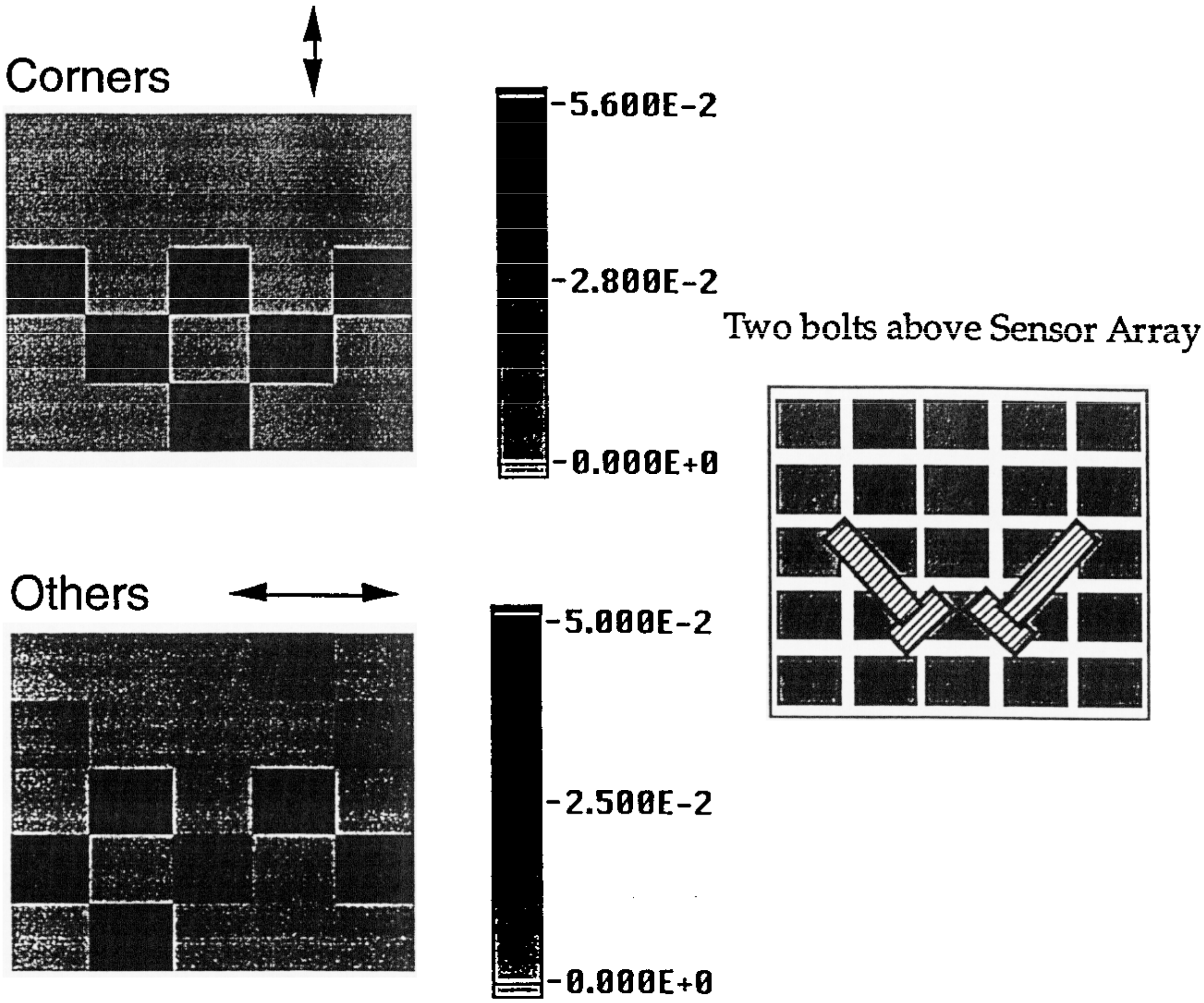

Figure 7. Image of two ferrous bolts placed above the array. The outline of the bolts is not directly visible, but the symmetry of the pattern is recognizable. More GMR elements and concomitant higher spatial resolution could substantially improve this image.

the various multipole components of the magnetization pattern. One must keep in mind that the magnetic field emanating from an object can vary in all three dimensions, and there is no particular reason in the absence of an external applied field for the symmetry of a 2D slice taken at one height to be exactly the same as a 2D slice taken at another height. On the other hand, the images sometimes appear rather simple, as in Figure 4. Intelligent synthesis of data and interpretation of images will be the major challenge in building a useful GMR-based UXO detector, although the intrinsic difficulty is not greater than in time-domain analysis of pulsed electromagnetic induction data, for example.

REALIZATION OF A FIELDABLE UXO DETECTION SYSTEM

There are several obvious improvements that would be necessary for a real-world UXO detector. For example, there are questions about portability and ruggedness of a fieldable GMR array system. In this regard it is worth noting that the power consumption per GMR sensor (about 5 mW dc for the NVS5B15) is quite reasonable. This amount of powe can be provided by a battery pack in a portable unit.

It should be clear from examination of the images that having a larger array with additional sensors will produce a more immediately recognizable result. There are no serious practical problems with constructing a larger array. Ideally the individual elements of a large array would be addressable via row and column transistors, much like a random-access memory or charge-coupled device array. Since UXO objects tend to be many centimeters in extent, the GMR elements in the proposed detector can be spaced far enough apart that there is plenty of printed-circuit board area available for these other electronic components.

For this demonstration, no signal conditioning electronics were employed; the sensors are wired directly to the data acquision card. A portable system with integrated field-producing coils and 3-axis sensitivity will require considerably more sophisticated signal conditioning and processing electronics. Since signal levels, data rates, and data amounts are all moderate for this application, design of the support electronics for a GMR detector should be straightforward. The implementation of UXO-recognition software is more ambitious since magnetic pattern recognition for extended objects is still a new field.

Finally it is worth noting that NVE's NVS sensors are the very first GMR-based products to be commercially available; GMR was only discovered in 1988. More sensitive GMR elements are expected to be available commercially later this year, with substantial improvement in sensor performance expected in the near future.

Part of this work was performed under the auspices of the U.S. Department of Energy by Lawrence Livermore National Laboratory under contract number W-7405-ENG-48. Thanks are due to John Anderson and Russell Beech of NVE and Gary Johnson and Alan Wiltse of LLNL for assistance with this project. Financial support was provided by the Program Development Office of the Chemistry and Materials Science Department at LLNL.

REFERENCES

Allen, G., R. Koch and G. Keefe, UXO Forum '96 Conference Proceedings, Williamsburg, VA, p. 1.

Anthony, T.C., J. A. Brug, and S. Zhang, "Magnetoresistance of Symmetric Spin Valve Structures," IEEE Trans. Magn. **30**, 3819 (1994).

Baibich, M.N. *et al.*, "Giant Magnetoresistance of (001) Fe/(001) Cr Magnetic Superlattices," Phys. Rev. Lett. **61**, 2472 (1988).

Binasch, G., P. Grünberg, F. Saurenbach and W. Zinn, "Enhanced magnetoresistance in layered magnetic structures with antiferromagnetic interlayer exchange," Phys. Rev. **B 39**, 4828 (1989).

Chaiken, A., G.A. Prinz, and J.J. Krebs, "Magnetotransport Study of Fe-Cr-Fe Sandwiches Grown on ZnSe," J. Appl. Phys. **67**, 4892 (1990).

Chaiken, A., P. Lubitz, J.J. Krebs, G.A. Prinz and M.Z. Harford, "Spin-Valve Magnetoresistance Of Uncoupled Fe-Cu-Co Sandwiches," J. Appl. Phys. **70**, 5864 (1991).

Kano, H., *et al.*, "Substrate Temperature Effect on Giant Magnetoresistance of Sputtered Co/Cu Multilayers," Appl. Phys. Lett. **63**, 2839 (1993).

McGlone, T.D., Proc. Symp. Applications of Geophysics and Engineering to Environmental Problems, Reno, NV, 1997, p. 705.

Nonvolatile Electronics (NVE) Inc., 11409 Valley View Road, Eden Prairie, MN 55344-3617, (800) 467-7141, http://www.nve.com, info@nve.com.

Technical Information Department **• Lawrence Livermore National Laboratory**
University of California • Livermore, California 94551